

Modified fuzzy rough set technique with stacked autoencoder model for magnetic resonance imaging based breast cancer detection

Sachin Kumar Mamdy¹, Vishwanath Petli²

¹Department of Electronics and Communication Engineering, VTU RRC, Visvesvaraya Technological University, Belagavi, India

²Department of Electronics and Communication Engineering, SLN College of Engineering, Raichur, India

Article Info

Article history:

Received Jul 9, 2023

Revised Jul 8, 2023

Accepted Jul 17, 2023

Keywords:

Breast cancer detection

Fuzzy rough set

Image enhancement

Magnetic resonance imaging

Otsu thresholding

Stacked autoencoder

ABSTRACT

Breast cancer is the common cancer in women, where early detection reduces the mortality rate. The magnetic resonance imaging (MRI) images are efficient in analyzing breast cancer, but it is hard to identify the abnormalities. The manual breast cancer detection in MRI images is inefficient; therefore, a deep learning-based system is implemented in this manuscript. Initially, the visual quality improvement is done using region growing and adaptive histogram equalization (AHE), and then, the breast lesion is segmented by Otsu thresholding with morphological transform. Next, the features are extracted from the segmented lesion, and a modified fuzzy rough set technique is proposed to reduce the dimensions of the extracted features that decreases the system complexity and computational time. The active features are fed to the stacked autoencoder for classifying the benign and malignant classes. The results demonstrated that the proposed model attained 99% and 99.22% of classification accuracy on the benchmark datasets, which are higher related to the comparative classifiers: decision tree, naïve Bayes, random forest and k-nearest neighbor (KNN). The obtained results state that the proposed model superiorly screens and detects the breast lesions that assists clinicians in effective therapeutic intervention and timely treatment.

This is an open access article under the [CC BY-SA](https://creativecommons.org/licenses/by-sa/4.0/) license.



Corresponding Author:

Sachin Kumar Mamdy

Department of Electronics and Communication Engineering, VTU RRC, Visvesvaraya Technological University

Belagavi, India

Email: msachin834@gmail.com

1. INTRODUCTION

In the current scenario, breast cancer is the common cancer type in the rural and urban areas, where women between the age group of thirty-fifty years are at a higher risk of breast cancer [1], [2]. It is the second most cause of cancer deaths in women after lung cancer [3]. Hence, the death rate of women due to breast cancer is 1 in 37 subjects, which is around 2.7%. Therefore, the proper treatment and early diagnosis of breast cancer are essential for decreasing the death rates and preventing the disease progression [4]–[6]. In recent decades, magnetic resonance imaging (MRI) images are highly utilized for diagnosing breast cancer to decrease unnecessary biopsies [7], [8]. Additionally, the MRI images are a highly recommended test to monitor and detect the breast cancer lesion and to interpret the lesioned region, because it has better soft tissue imaging [9]. Additionally, an experienced physician is needed to process the MRI images, which is a time-consuming mechanism [10], [11]. For overcoming the above-stated issue, several automated models are

implemented by the researchers [12], [13]. Singh *et al.* [14] introduced a novel two-stage model for tumor classification. The integration of adversarial network and convolutional neural network (CNN) requires a large amount of medical data for training the developed model, which was extremely expensive. Ibraheem *et al.* [15] combined two dimensional median filter and discrete wavelet transform for improving the quality of breast images and extracting the features. The extracted features were given to the support vector machine (SVM) for tumor and healthy region classification. The SVM does not work well, when the target-classes were overlapping and the collected data was noisier. Khan *et al.* [16] introduced a deep learning framework based on the concept of transfer learning for breast cancer detection. In the presented deep learning system, three pre-trained models like residual network (ResNet), GoogLeNet and visual geometry group network (VGGNet) were used to extract features from the breast cytology images. The extracted deep learning features were fed to the fully connected layer of the transfer-learning model for malignant and benign classification. The developed transfer-learning model needs expensive graphics processing unit systems that increase computational cost.

Ragab *et al.* [17] has integrated ResNet, AlexNet, and GoogLeNet models for extracting deep features from the breast mammogram images. The extracted features were given to the SVM classifier for tumor and non-tumor region classification. However, the SVM classifier was suitable for binary class classification, where it was inappropriate for multiclass classification. On the other hand, Alanazi *et al.* [18] has presented a CNN model for boosting the automatic detection of cancer regions by utilizing histopathology images, where it was computationally expensive. Fang *et al.* [19] firstly applied median filtering technique for enhancing the quality of mammogram images. Then, the whale optimization algorithm was combined with the multilayer perceptron algorithm for classifying the breast images as healthy or cancerous. The evaluation outcomes demonstrated that the presented model obtained higher accuracy than the existing models. The multilayer perceptron algorithm was sensitive to feature scaling and needs more hyper-parameters tuning such as hidden layers and neurons. Gravina *et al.* [20] developed a CNN model based on the intrinsic deforming autoencoders for automatic breast lesion malignancy recognition. The CNN was computationally costly, where it requires an enormous amount of data in order to obtain better classification results. Chouhan *et al.* [21] developed a deep highway network to extract dynamic features from the digital breast mammogram images. Further, the extracted features were given to the SVM and emotional learning inspired ensemble model for benign and malignant classification. As specified earlier, the developed SVM model supports only binary class classification.

Khamparia *et al.* [22] has implemented a hybrid transfer-learning model that combines ImageNet and modified VGGNets for superior breast cancer recognition. The presented hybrid transfer-learning model was a superior tool for clinicians in order to diminish the false positive and false negative rates of breast cancer recognition, but it was computationally complex. In addition, Yurttakal *et al.* [23] implemented a time saving deep CNN model for classifying the breast lesions as benign or malignant tumors. The presented time saving deep CNN model obtained promising results in the breast cancer classification by means of specificity, accuracy, and sensitivity. In addition, Hizukuri *et al.* [24] developed a deep CNN model with Bayesian optimization for effective breast cancer classification. As presented in the resulting section, the deep CNN model obtained higher classification performance and it would be useful in early diagnoses of breast masses. However, the vanishing gradients was a major problem in the hybrid transfer-learning model and deep CNN model. To highlight the above-stated issues and to enhance breast-cancer detection, a novel deep learning system is implemented in this work. The primary aim of this article is to categorize the malignant and benign breast lesions with limited system complexity and computational time. The contributions are listed below:

- After acquiring the breast images from breast imaging-reporting and data system (BI-RADS) MRI and breast dynamic contrast material-enhanced MRI (DCE-MRI) datasets, the image denoising is carried out by using region growing and adaptive histogram equalization (AHE) techniques. The undertaken pre-processing techniques significantly enhance the edge definitions and improve the local contrast of the collected breast images.
- The breast lesion segmentation is accomplished utilizing Otsu thresholding with morphological transform, where this technique is effective, when the background condition is unchanged.
- The discriminative features are extracted from the segmented lesions by utilizing local ternary pattern (LTP) and steerable pyramid transform (SPT). Then, the dimensions of the extracted features are diminished by proposing a modified fuzzy rough set technique that enhances the computational time and complexity of the stacked autoencoder model, which is used for classification. The modified fuzzy rough set technique combines the fuzzy equivalence and the membership function of fuzzy c means clustering technique for feature optimization. The rough set based stacked autoencoder model's effectiveness is analyzed in terms of positive predicted value (PPV), specificity, accuracy, negative predicted value (NPV), and sensitivity.

This article is arranged in the following manner; the proposed methodology explanations are described in section 2. The simulation outcomes and its comparison are demonstrated in section 3. Finally, the conclusion of this study is depicted in section 4.

2. METHOD

In the context of breast cancer detection, the presented deep-learning framework comprises six phases. These six phases include image acquisition: BI-RADS MRI and DCE-MRI datasets, image denoising: region growing and adaptive histogram equalization, segmentation: Otsu thresholding with morphological transform, feature extraction: steerable pyramid transform and local ternary pattern descriptor, feature optimization: modified fuzzy rough set, and classification: stacked autoencoder. The workflow of the developed deep learning framework is represented in Figure 1.

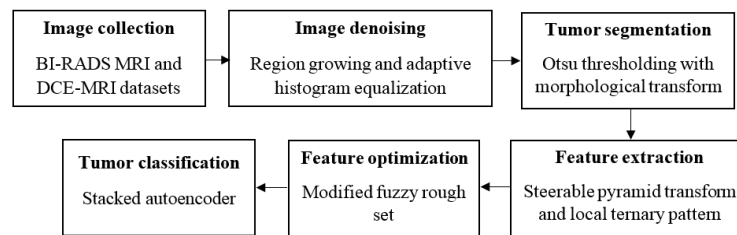


Figure 1. Workflow of the developed deep learning framework

2.1. Image acquisition and denoising

In this research work, the developed deep learning framework's effectiveness is validated using the BI-RADS MRI and DCE-MRI datasets. The BI-RADS MRI dataset consists of 200 MRI breast images in that 98 breast images are benign and 102 breast images are malignant. In the BI-RADS MRI dataset, the benign breast images are 17.63 ± 5.79 mm in size and the malignant breast images are 29.80 ± 9.88 mm in size. In addition, the subjects with granulomatous mastitis and infection are excluded from the research. Table 1 states the data statistics of the BI-RADS MRI dataset. On the other hand, the DCE-MRI dataset comprises 56 MRI examinations of 56 patients in which 30 are malignant masses and 26 are benign masses. The sample-acquired images are denoted in Figure 2.

Table 1. Data statistics of the BI-RADS MRI dataset

Sequence	Contrast enhanced subtracted images
Image resolution	288×288
Image format	DICOM
Malignant	102
Benign	98
Slice thickness	<2.0 mm
Cases	200

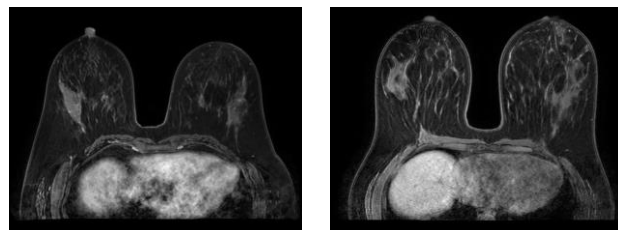


Figure 2. Sample acquired images

After collecting the raw breast MRI images, the pre-processing is carried out by utilizing AHE technique and region growing. Firstly, the AHE is an effective image processing technique, which is

employed to enhance the contrast of the raw breast MRI images. The AHE technique computes different histogram values to distinguish the images into many sections and then utilizes these sections for redistributing the lightness of the breast MRI images. Hence, the AHE technique is appropriate to enhance the image edges and to improve the local contrast of the collected breast MRI images [25]. Additionally, the region growing technique completely relies on the neighborhood image pixel assumption [26]. The region growing techniques compare one pixel with the neighbourhood pixels. If the similarity criterion is satisfied, the pixels belong to the clusters. The output image of the AHE and region-growing techniques are graphically depicted in Figures 3 and 4.

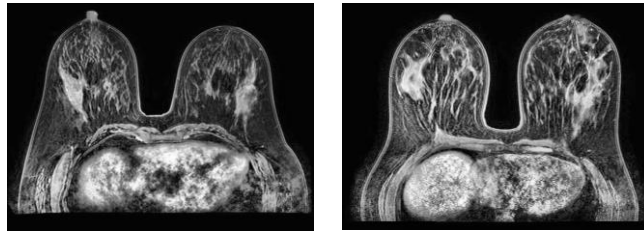


Figure 3. Output images of AHE technique

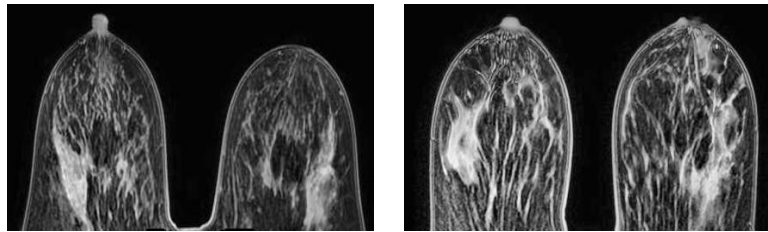


Figure 4. Output images of region growing

2.2. Tumor segmentation

After denoising the breast images, the tumor segmentation is accomplished by utilizing Otsu thresholding technique. The Otsu thresholding is an effective and simple segmentation technique, where it uses maximum class variance values. Related to existing image segmentation techniques, the Otsu thresholding technique includes advantages like need only smaller storage space, faster processing speed and ease in implementation. The pixel intensity level of the denoised image L is initially determined by utilizing (1).

$$PH_i^e = \frac{H_i^e}{M}, \sum_{i=1}^M PH_i^e = 1, e = \begin{cases} 1, 2, 3 & \text{if RGB} \\ 1 & \text{if grayscale} \end{cases} \quad (1)$$

where, H_i^e indicates the pixel intensity value that corresponds to the intensity levels from i until e , and PH_i^e represents distribution probability value of the denoised image. Additionally, E indicates image components (grayscale or RGB) and M specifies the number of pixel values in the denoised breast images [27]. Next, the histogram values in the probability distribution are normalized using (2).

$$w_0^E(th) = \sum_{i=1}^{th} PH_i^e, w_1^E(th) = \sum_{i=th+1}^L PH_i^e \quad (2)$$

where, $E_1 = \frac{PH_1^e}{w_0^E(th)}, \dots, \frac{PH_{th}^e}{w_0^E(th)}$, $E_2 = \frac{PH_{th+1}^e}{w_1^E(th)}, \dots, \frac{PH_L^e}{w_1^E(th)}$, $w_0(th)$ and $w_1(th)$ denotes probability distribution from E_1 and E_2 . Further, calculate the variants and average levels between the classes C by utilizing the (3) and (4).

$$\mu_0^e = \sum_{i=1}^{th} \frac{iPH_i^e}{w_0^E(th)}, \mu_1^e = \sum_{i=th+1}^L \frac{iPH_i^e}{w_1^E(th)}, \quad (3)$$

$$\sigma^{2e} = \sigma_1^e + \sigma_2^e, \quad (4)$$

where, $\sigma_1^e = w_0^e(\mu_0^e + \mu_T^e)^2$, $\sigma_2^e = w_1^e(\mu_1^e + \mu_T^e)^2$, σ^{2e} represents variants between the classes C (benign and malignant classes), σ_1^e and σ_2^e denotes class variants one and two, and μ_0^e and μ_1^e states average rate for the class variants one and two. Then, the objective function is calculated utilizing (5).

$$J(th) = \max(\sigma^{2e}(th)), 0 \leq th_i \leq L - 1, i = 1, 2, 3, \dots K \quad (5)$$

where, $th = th_1, th_2, \dots, th_{K-1}$ represents a vector, which contains multiple thresholds. The Otsu thresholding between the class variance function is maximized to achieve the optimum threshold level of breast image for better tumor segmentation by increasing the objective function. In addition, the morphological dilation operator is employed on the output images of the Otsu thresholding technique that utilizes a structural element for expanding and probing the shapes in the output images of the Otsu thresholding technique. The output images of Otsu thresholding with morphological transform are graphically represented in Figure 5.

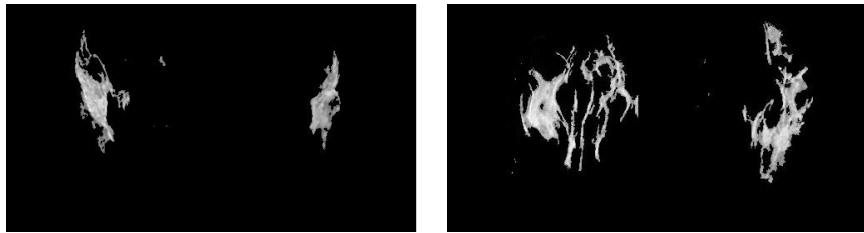


Figure 5. Output images of Otsu thresholding with morphological transform

2.3. Feature extraction with optimization

After tumor segmentation, the feature extraction is performed by utilizing steerable pyramid transform (SPT) and local ternary pattern (LTP) for extracting the features from the segmented tumor regions. The SPT is a linear multi-orientation and multi-scale image decomposition method, where the major portions of the linear transforms are sub-band transforms. Initially, the SPT is an effective image decomposition method that partitions the segmented tumor images into numerous sub-bands using orientation and scale, which is calculated using decimation and convolution operations. The sub-bands of the SPT are rotation invariant and translation that reduce the concern of orthogonal-separable-wavelet-decomposition [28]. In the SPT method, the segmented image is partitioned into low and high pass sub-bands utilizing the filters $L0$ and $H0$. Further, the low pass sub-bands are decomposed into four oriented band-pass sub-bands utilizing low pass filter $L1$ and band pass filters $B0$, $B1$, $B2$, and $B3$. Lastly, a robust image representation is generated with high orientation and scale by increasing the number of pyramid levels and number of image orientations.

Additionally, the LTP is a three-value texture descriptor for extracting the textual feature vectors from the segmented images. The LTP labels the image pixels with a threshold value by multiplying and adding the centre neighborhood image pixels p_c to generate the new labels. After defining the threshold value t , the pixel values within the range of $-t$ to $+t$ are considered to assign the value of zero to the image pixels [29]. The value 1 is assigned to the image pixels, if the value is higher than the threshold value, and the value -1 is assigned to the image pixels if the value is lower than the center pixel value. The mathematical expression of the LTP operator is represented in (6).

$$LTP = \begin{cases} 1 & \text{if } p_i - p_c \geq t \\ 0 & \text{if } |p_i - p_c| < t \\ -1 & \text{if } p_i - p_c \leq -t \end{cases} \quad (6)$$

where, t indicates user-specified threshold, p_i denotes neighborhood pixel value and p_c represents a central pixel value. The hybrid feature extraction (LTP and SPT) extracts 1536 features from the segmented images. The dimensions of the extracted feature vectors are decreased by implementing the modified fuzzy rough set technique. Generally, the fuzzy rough set utilizes two approximations such as lower and upper limits for feature optimization that ranges between $[0, 1]$. The conventional fuzzy rough set feature optimization is employed on nominal, valued, continuous and nominal data, where it significantly handles the data noise. Several reformulations are carried out in a fuzzy rough set to speed up the calculations. In this manuscript,

the modified fuzzy rough set technique is proposed that integrates the fuzzy equivalence and the membership function of fuzzy c means clustering technique for feature optimization. The modified fuzzy rough set technique knows the dataset and selects the highly correlated feature vectors of 537 for disease classification. The flowchart of the modified fuzzy rough set technique is represented in Figure 6.

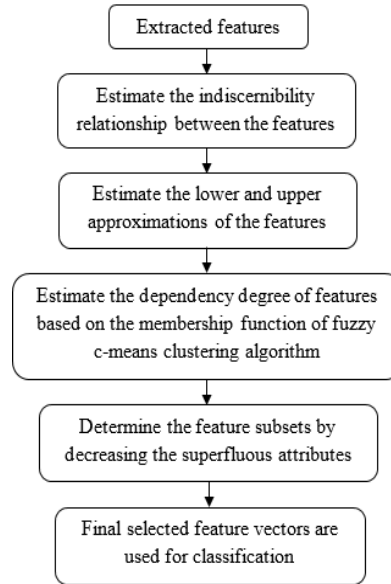


Figure 6. Flowchart of the modified fuzzy rough set technique

2.4. Classification

After choosing the active features, the stacked autoencoder is applied for classification [30]. The stacked autoencoder classification technique comprises multi-layer autoencoders that obtain higher-level representation of the original feature vectors by reconstructing input and its structure. In the input layer, the original information is encoded for obtaining the higher-level feature vectors of the middle-hidden layer and then the input information is reconstructed by decoding the information. By minimizing the reconstruction error, the stacked autoencoder networks are trained. The original training data is considered as x and the hidden layer is mathematically expressed in (7).

$$y^{(i)} = f(W_1^T x^{(i)} + b^2) \quad (7)$$

where $f = \tanh(\cdot)$ represents activation function. Further, the output z is obtained by decoding the original information, which is mathematically represented in (8). Then, the objective is minimized for training the autoencoder that is defined in (9).

$$z^{(i)} = W_2^T y^{(i)} + b^2 \approx x^{(i)} \quad (8)$$

$$J(X, Z) = \frac{1}{2} \sum_{i=1}^M \|x^{(i)} - z^{(i)}\|^2 \quad (9)$$

The stacked autoencoder is trained on the basis of layer-by-layer greedy method. Particularly, the feature vector of the upper hidden layer is used as the input of the succeeding layers, which is named as pre-training. Further, the weights of the pre-trained network are connected and then the weights of the final network are obtained by fine-tuning. The assumed parameters are: maximum iterations: softmax learning is 100, sparsity proportion is 0.15, maximum iterations: SAE learning is 100, L2 weight regularization is 0.004, sparsity regularization is 4, and a number of hidden layers is 100.

3. RESULTS AND DISCUSSION

In the automated breast cancer detection, the developed rough set based stacked autoencoder model's efficacy is simulated by MATLAB 2020. The rough set based stacked autoencoder model's efficacy

is analyzed in terms of PPV, specificity, accuracy, NPV and sensitivity on the BI-RADS MRI and DCE-MRI datasets. However, the NPV and PPV are defined as the proportions of the negative and positive results in the statistic and diagnostic tests, which are true negative and true positive results. The formulae of NPV and PPV are depicted in equations (10) and (11).

$$NPV = \frac{TN}{TN+FN} \times 100 \quad (10)$$

$$PPV = \frac{TP}{TP+FP} \times 100 \quad (11)$$

The sensitivity is a test that determines the patient cases precisely and the specificity is a test that precisely identifies the healthy cases. In addition, accuracy is a vital evaluation metric in breast cancer detection that indicates how closer the obtained results are to the actual results. The mathematical formulae of sensitivity, specificity and accuracy are stated in (12), (13), and (14). Where, FP, TP, FN, and TN indicate false positive, true positive, false negative and true negative values.

$$Accuracy = \frac{TP+TN}{TP+TN+FP+FN} \times 100 \quad (12)$$

$$Specificity = \frac{TN}{TN+FP} \times 100 \quad (13)$$

$$Sensitivity = \frac{TP}{TP+FN} \times 100 \quad (14)$$

3.1. Quantitative analysis

In this scenario, the rough set based stacked autoencoder model's efficacy is analysed on the BI-RADS MRI dataset that comprises 200 MRI breast images in which 20% breast images are utilized for model testing. Additionally, the proposed rough set based stacked autoencoder model is evaluated by a five-fold cross validation technique that diminishes the computational time, and the variance of the estimated parameters against the dataset. In Table 2, the experimental analysis is carried-out utilizing different classifiers such as stacked autoencoder, naïve Bayes, random forest (RF), decision tree (DT), and k-nearest neighbor (KNN) along with and without feature optimization in that the combination: a modified fuzzy rough set technique with stacked autoencoder obtained maximum performance with sensitivity of 98.68%, PPV of 98.11%, classification accuracy of 99%, specificity of 99%, and NPV of 97.56% on the BI-RADS MRI dataset. The experimental outcome by changing the classifiers with and without feature optimization is represented in Figures 7 and 8.

Table 2. Experimental result by changing the classifiers on the BI-RADS MRI dataset

	Classifier	Accuracy (%)	Sensitivity (%)	Specificity (%)	PPV (%)	NPV (%)
Without feature optimization	KNN	81.14	80.44	79.94	80.69	79.71
	Random forest	86.24	85.81	83.71	87.78	83.75
	Naïve Bayes	90.45	90.57	89.34	91.79	89.25
	Decision tree	85.94	82.99	86.03	85.22	86.27
	Stacked autoencoder	95.62	96.31	96.78	94.56	94.77
With feature optimization	KNN	82.50	84.29	83.26	82.11	81.43
	Random forest	88.22	89.55	90.10	88.53	88.31
	Naïve Bayes	92.74	93.88	93.84	91.55	93.32
	Decision tree	90.98	91.57	89.01	89.99	92.30
	Stacked autoencoder	99	98.68	99	98.11	97.56

Table 3 reveals that the modified fuzzy rough set technique with stacked autoencoder achieved maximum classification performance in the breast cancer detection on the BI-RADS MRI dataset related to other optimizers like artificial bee colony (ABC), particle swarm optimizer (PSO), and grey wolf optimizer (GWO). In this research manuscript, the modified fuzzy rough set technique is significant for visualization and feature optimization of the BI-RADS MRI dataset, where it effectively deals with the hybrid decision systems. The experimental results by varying the feature optimizers are graphically stated in Figure 9.

Similar to the BI-RADS MRI dataset, the proposed rough set based stacked autoencoder has obtained higher classification accuracy of 99.22%, sensitivity of 98.80%, specificity of 98.91%, PPV of 98.92%, and NPV of 98.90% on the DCE-MRI dataset. The achieved experimental results are maximum related to other classifiers and optimizers, as specified in Tables 4 and 5.

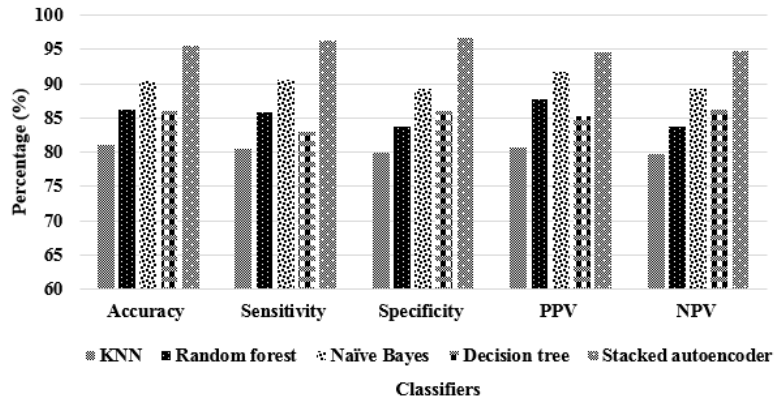


Figure 7. Comparison result by changing the classifiers without feature optimization on the BI-RADS MRI dataset

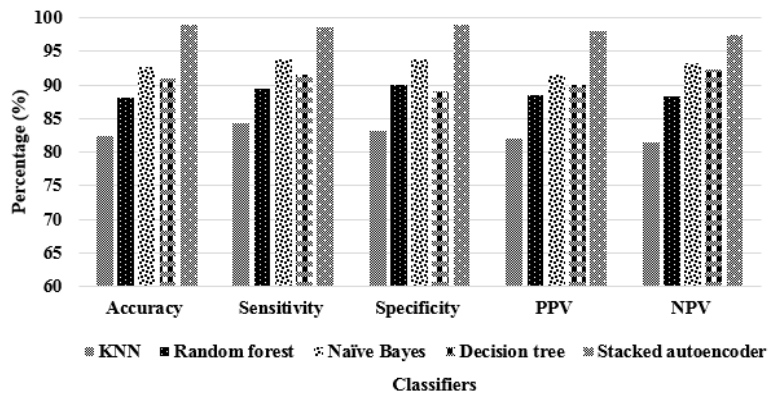


Figure 8. Comparison result by changing the classifiers with feature optimization on the BI-RADS MRI dataset

Table 3. Experimental result by changing the feature optimizers on the BI-RADS MRI dataset

Stacked autoencoder					
Optimizers	Accuracy (%)	Sensitivity (%)	Specificity (%)	PPV (%)	NPV (%)
PSO	88.35	88.11	88.72	88.37	87.11
GWO	92.29	92.54	92.86	91.70	92.60
ABC	95.24	96.56	94.71	96.72	94.59
Modified fuzzy rough set	99	98.68	99	98.11	97.56

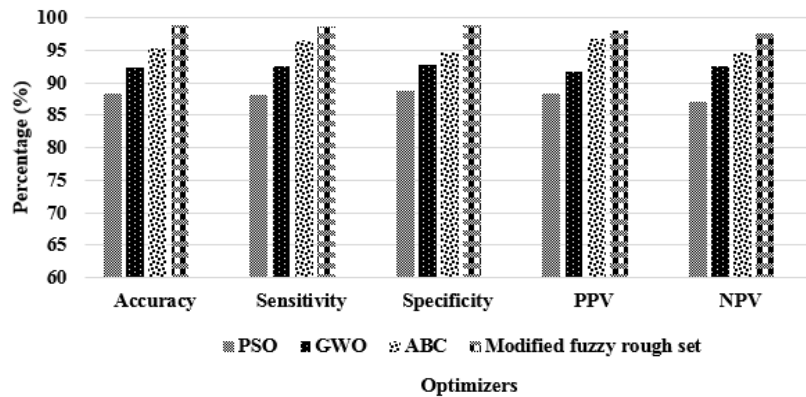


Figure 9. Comparison result by changing the feature optimizers with stacked autoencoder on the BI-RADS MRI dataset

Table 4. Experimental result by changing the classifiers on the DCE-MRI dataset

	Classifier	Accuracy (%)	Sensitivity (%)	Specificity (%)	PPV (%)	NPV (%)
Without feature optimization	KNN	82.65	82.11	81.90	85.65	84.70
	Random forest	84.32	86.78	85.70	89.90	88.22
	Naïve Bayes	93.22	90.99	89	90.11	90.25
	Decision tree	94.34	93.21	90.08	92.90	90.33
	Stacked autoencoder	95.80	95.65	93.77	95.50	93.70
With feature optimization	KNN	90.33	90.90	91.28	90.12	91.40
	Random forest	92.38	93.10	92.10	95.50	92.99
	Naïve Bayes	96.70	95.84	93.99	96.86	94.34
	Decision tree	97.07	96.50	95.08	97.90	96.30
	Stacked autoencoder	99.22	98.80	98.91	98.92	98.90

Table 5. Experimental result by changing the feature optimizers on the DCE-MRI dataset

Optimizers	Stacked autoencoder				
	Accuracy (%)	Sensitivity (%)	Specificity (%)	PPV (%)	NPV (%)
PSO	93.38	90.11	90.70	90.30	91.32
GWO	94.20	94.84	94.85	92.62	93.68
ABC	95.08	96.40	95.09	93.88	94.11
Modified fuzzy rough set	99.22	98.80	98.91	98.92	98.90

3.2. Comparative analysis

The comparative results of the prior models and the rough set based stacked autoencoder model is represented in Table 6. Yurttakal *et al.* [23] presented a deep CNN model for classifying the breast MRI lesions as malignant and benign. The simulation outcomes demonstrated that the deep CNN model achieved 98.33% of classification accuracy and 96.88% of specificity on the BI-RADS MRI dataset. In addition, Hizukuri *et al.* [24] integrated a deep CNN model with Bayesian optimization for effective breast cancer classification. As depicted in the resulting section, the developed model obtained 92.90% of accuracy and 92.30% of specificity on the DCE-MRI dataset. Compared to the existing deep CNN models, the rough set based stacked autoencoder model obtained superior performance in breast lesion detection by means of different evaluation measures.

Table 6. Comparative evaluation between the existing and the proposed rough set based stacked autoencoder model

Models	Dataset	Accuracy (%)	Specificity (%)
Deep CNN [23]	BI-RADS MRI	98.33	96.88
Deep CNN with Bayesian optimization [24]	DCE-MRI	92.90	92.30
Rough set based stacked autoencoder model	BI-RADS MRI	99	99
	DCE-MRI	99.22	98.91

3.3. Discussion

The segmentation, feature optimization, and classification are the vital parts of this research for precise breast cancer detection with minimal computational time. The Otsu thresholding with morphological transform is simple and speed in finding the optimal threshold value for separating foreground and background regions. After feature extraction, the incorporation of the modified fuzzy rough set technique in the proposed system diminishes the computational time and complexity of the stacked autoencoder by selecting active features. The computational complexity of the rough set based stacked autoencoder model is linear $O(N)$, where O indicates the order of magnitude and N states input size. The proposed model consumes 34 and 22 seconds to train and test the BI-RADS MRI and DCE-MRI datasets, which are minimum related to other comparative classification models. Additionally, the stacked autoencoder easily and effectively learns non-linear transformation with multiple layers and activation functions for better disease classification. The computational complexity and training time are the major issues addressed in the related work section that are effectively overcome by the rough set based stacked autoencoder model.

4. CONCLUSION

In this manuscript, a new rough set based stacked autoencoder model is implemented for effective breast cancer detection. The aim of this research is to develop a feature optimizer and an effective deep learning classifier for effective classification of breast cancer. Therefore, the most pre-dominant

discriminative feature vectors are selected utilizing the modified fuzzy rough set technique. Further, the selected features are given as the input to the stacked autoencoder for classifying both the malignant and benign breast lesions. The proposed rough set based stacked autoencoder model delivers superior performance in the breast cancer recognition in terms of classification accuracy, PPV, specificity, NPV, and sensitivity. In the experimental segment, the proposed rough set based stacked autoencoder model obtained classification accuracy of 99% and 99.22% on the BI-RADS MRI and DCE-MRI datasets. The obtained experimental outcomes are superior to the conventional classifiers and optimizers. Breast cancer detection by the proposed rough set based stacked autoencoder model can assist doctors and pathologists in the classification of abnormalities with maximum accuracy in minimal computational time. In future, a new ensemble based deep learning model can be included in the proposed system to further detect the sub-stages of breast cancer.

AUTHOR CONTRIBUTIONS

For this research work all authors' have equally contributed in Conceptualization, methodology, validation, resources, writing-original draft preparation, writing-review and editing.




REFERENCES

- [1] R. Beňačka, D. Szabóová, Z. Guľašová, Z. Hertelyová, and J. Radoňák, "Classic and new markers in diagnostics and classification of breast cancer," *Cancers*, vol. 14, no. 21, Nov. 2022, doi: 10.3390/cancers14215444.
- [2] H. Aljuaid, N. Alturki, N. Alsubaie, L. Cavallaro, and A. Liotta, "Computer-aided diagnosis for breast cancer classification using deep neural networks and transfer learning," *Computer Methods and Programs in Biomedicine*, vol. 223, Aug. 2022, doi: 10.1016/j.cmpb.2022.106951.
- [3] M. I. Daoud, S. Abdel-Rahman, T. M. Bdaif, M. S. Al-Najar, F. H. Al-Hawari, and R. Alazrai, "Breast tumor classification in ultrasound images using combined deep and handcrafted features," *Sensors*, vol. 20, no. 23, Nov. 2020, doi: 10.3390/s20236838.
- [4] T. R. Mahesh, V. V. Kumar, V. Vivek, K. M. K. Raghunath, and G. S. Madhuri, "Early predictive model for breast cancer classification using blended ensemble learning," *International Journal of System Assurance Engineering and Management*, Jun. 2022, doi: 10.1007/s13198-022-01696-0.
- [5] G. Murtaza, L. Shuib, A. W. A. Wahab, G. Mujtaba, and G. Raza, "Ensembled deep convolution neural network-based breast cancer classification with misclassification reduction algorithms," *Multimedia Tools and Applications*, vol. 79, no. 25–26, pp. 18447–18479, Jul. 2020, doi: 10.1007/s11042-020-08692-1.
- [6] O. J. Egwom, M. Hassan, J. J. Tanimu, M. Hamada, and O. M. Ogar, "An LDA–SVM machine learning model for breast cancer classification," *BioMedInformatics*, vol. 2, no. 3, pp. 345–358, Jun. 2022, doi: 10.3390/biomedinformatics2030022.
- [7] S. Boumaraf, X. Liu, C. Ferkous, and X. Ma, "A new computer-aided diagnosis system with modified genetic feature selection for BI-RADS classification of breast masses in mammograms," *BioMed Research International*, vol. 2020, pp. 1–17, May 2020, doi: 10.1155/2020/7695207.
- [8] D. Sheth and M. L. Giger, "Artificial intelligence in the interpretation of breast cancer on MRI," *Journal of Magnetic Resonance Imaging*, vol. 51, no. 5, pp. 1310–1324, May 2020, doi: 10.1002/jmri.26878.
- [9] M. Desai and M. Shah, "An anatomization on breast cancer detection and diagnosis employing multi-layer perceptron neural network (MLP) and convolutional neural network (CNN)," *Clinical eHealth*, vol. 4, pp. 1–11, 2021, doi: 10.1016/j.ceh.2020.11.002.
- [10] B. V. Divyashree and G. H. Kumar, "Breast cancer mass detection in mammograms using gray difference weight and MSER detector," *SN Computer Science*, vol. 2, no. 2, Apr. 2021, doi: 10.1007/s42979-021-00452-8.
- [11] Y. Shen *et al.*, "An interpretable classifier for high-resolution breast cancer screening images utilizing weakly supervised localization," *Medical Image Analysis*, vol. 68, Feb. 2021, doi: 10.1016/j.media.2020.101908.
- [12] M. Pavithra, R. Rajmohan, T. A. Kumar, and R. Ramya, "Prediction and classification of breast cancer using discriminative learning models and techniques," in *Machine Vision Inspection Systems, Volume 2*, Wiley, 2021, pp. 241–262.
- [13] N. M. ud Din, R. A. Dar, M. Rasool, and A. Assad, "Breast cancer detection using deep learning: Datasets, methods, and challenges ahead," *Computers in Biology and Medicine*, vol. 149, Oct. 2022, doi: 10.1016/j.combiomed.2022.106073.
- [14] V. K. Singh *et al.*, "Breast tumor segmentation and shape classification in mammograms using generative adversarial and convolutional neural network," *Expert Systems with Applications*, vol. 139, Jan. 2020, doi: 10.1016/j.eswa.2019.112855.
- [15] A. M. Ibraheem, K. H. Rahouma, and H. F. A. Hamed, "Automatic MRI Breast tumor detection using discrete wavelet transform and support vector machines," in *2019 Novel Intelligent and Leading Emerging Sciences Conference (NILES)*, Oct. 2019, pp. 88–91, doi: 10.1109/NILES.2019.8909345.
- [16] S. Khan, N. Islam, Z. Jan, I. Ud Din, and J. J. P. C. Rodrigues, "A novel deep learning based framework for the detection and classification of breast cancer using transfer learning," *Pattern Recognition Letters*, vol. 125, pp. 1–6, Jul. 2019, doi: 10.1016/j.patrec.2019.03.022.
- [17] D. A. Ragab, O. Attallah, M. Sharkas, J. Ren, and S. Marshall, "A framework for breast cancer classification using multi-DCNNs," *Computers in Biology and Medicine*, vol. 131, Apr. 2021, doi: 10.1016/j.combiomed.2021.104245.
- [18] S. A. Alanazi *et al.*, "Boosting breast cancer detection using convolutional neural network," *Journal of Healthcare Engineering*, pp. 1–11, Apr. 2021, doi: 10.1155/2021/5528622.
- [19] H. Fang, H. Fan, S. Lin, Z. Qing, and F. R. Sheykhahmad, "Automatic breast cancer detection based on optimized neural network using whale optimization algorithm," *International Journal of Imaging Systems and Technology*, vol. 31, no. 1, pp. 425–438, Mar. 2021, doi: 10.1002/ima.22468.
- [20] M. Gravina, S. Marrone, M. Sansone, and C. Sansone, "DAE-CNN: Exploiting and disentangling contrast agent effects for breast lesions classification in DCE-MRI," *Pattern Recognition Letters*, vol. 145, pp. 67–73, May 2021, doi: 10.1016/j.patrec.2021.01.023.
- [21] N. Chouhan, A. Khan, J. Z. Shah, M. Hussain, and M. W. Khan, "Deep convolutional neural network and emotional learning based breast cancer detection using digital mammography," *Computers in Biology and Medicine*, vol. 132, May 2021, doi: 10.1016/j.combiomed.2021.104318.




- [22] A. Khamparia *et al.*, “Diagnosis of breast cancer based on modern mammography using hybrid transfer learning,” *Multidimensional Systems and Signal Processing*, vol. 32, no. 2, pp. 747–765, Apr. 2021, doi: 10.1007/s11045-020-00756-7.
- [23] A. H. Yurttakal, H. Erbay, T. İkizceli, and S. Karaçavuş, “Detection of breast cancer via deep convolution neural networks using MRI images,” *Multimedia Tools and Applications*, vol. 79, no. 21–22, pp. 15555–15573, Jun. 2020, doi: 10.1007/s11042-019-7479-6.
- [24] A. Hizukuri, R. Nakayama, M. Nara, M. Suzuki, and K. Namba, “Computer-aided diagnosis scheme for distinguishing between benign and malignant masses on breast DCE-MRI images using deep convolutional neural network with bayesian optimization,” *Journal of Digital Imaging*, vol. 34, no. 1, pp. 116–123, Feb. 2021, doi: 10.1007/s10278-020-00394-2.
- [25] U. K. Acharya and S. Kumar, “Genetic algorithm based adaptive histogram equalization (GAAHE) technique for medical image enhancement,” *Optik*, vol. 230, Mar. 2021, doi: 10.1016/j.ijleo.2021.166273.
- [26] T. Sadad, A. Munir, T. Saba, and A. Hussain, “Fuzzy C-means and region growing based classification of tumor from mammograms using hybrid texture feature,” *Journal of Computational Science*, vol. 29, pp. 34–45, Nov. 2018, doi: 10.1016/j.jocs.2018.09.015.
- [27] Z. Y. Tan, S. N. Basah, H. Yazid, and M. J. A. Safar, “Performance analysis of Otsu thresholding for sign language segmentation,” *Multimedia Tools and Applications*, vol. 80, no. 14, pp. 21499–21520, Jun. 2021, doi: 10.1007/s11042-021-10688-4.
- [28] R. Biswas, S. Roy, and A. Biswas, “MRI and CT image indexing and retrieval using steerable pyramid transform and local neighborhood difference pattern,” *International Journal of Computers and Applications*, vol. 44, no. 11, pp. 1005–1014, Nov. 2022, doi: 10.1080/1206212X.2022.2092937.
- [29] M. O. Divya and E. R. Vimina, “Content based image retrieval with multi-channel LBP and colour features,” *International Journal of Applied Pattern Recognition*, vol. 6, no. 2, 2020, doi: 10.1504/IJAPR.2020.10033780.
- [30] M. Yu, T. Quan, Q. Peng, X. Yu, and L. Liu, “A model-based collaborate filtering algorithm based on stacked AutoEncoder,” *Neural Computing and Applications*, vol. 34, no. 4, pp. 2503–2511, Feb. 2022, doi: 10.1007/s00521-021-05933-8.

BIOGRAPHIES OF AUTHORS



Sachin Kumar Mamdy    completed B.E. from PDA college of Engineering, Kalaburagi under VTU, Belagavi in the year 2010 and completed M. Tech from JNTU Hyderabad in the year 2013. He has presented two papers in international conference. He can be contacted at email: msachin834@gmail.com.



Vishwanath Petli    completed his M.E from PDA Dcollege of Engineering, Gulbarga University, Gulbarga (Karnataka) in the year 2003 and completed his Ph. D. in the year 2017 from NIMS University, Jaipur (Rajasthan). Presently working as Associate Professor in the department of Electronics and Communication Engineering since 1998. His area of interest are image processing and embedded system. He has published four papers in international journals and presented one paper in international conference. He can be contacted at email: vishalpetli73@gmail.com.